

# Annual variation of sporadic radar meteor rates

M. D. Campbell-Brown<sup>★</sup> and J. Jones

*University of Western Ontario, London, ON N6A 3K7, Canada*

Accepted 2005 December 8. Received 2005 December 6; in original form 2005 October 25

## ABSTRACT

The activity of sporadic meteors has been measured from 2002 to 2005 with the Canadian Meteor Orbit Radar. Single-station data at 29.85 MHz have been used to find the positions of the five sporadic sources visible from the Northern hemisphere, and the activity measured for each source has been corrected for observing biases. Relative fluxes and the annual variation of each source are well determined. The variations in activity are of great interest in determining the history and origin of the sporadic meteoroid population.

**Key words:** meteors, meteoroids.

## 1 INTRODUCTION

Sporadic meteoroids, those that do not belong to known showers, make up the bulk of the meteoroids striking the Earth. They are thought to be a combination of both stoney particles produced in interasteroidal collisions and more fragile cometary particles. The action of planetary gravitational forces together with radiation forces have combined to reduce the coherence the initial orbits of these particles to such a degree that they have become so diffuse as to be no longer recognizable as streams and merge together into the sporadic meteoroid complex. But the sporadic background is not without structure. Several distinct areas of sporadic activity have been identified which come from well-defined directions relative to the sun. The helion and antihelion sources are in the plane of the ecliptic, and are located  $60^\circ$ – $70^\circ$  from the apex direction, near the helion and antihelion points. They were first discovered in an extensive radiant survey by the Jodrell Bank and Adelaide radars (Hawkins 1956; Weiss & Smith 1960). The apex source, which may be split into a north and south component (Sekanina 1976), is centred on the apex of the Earth's way. Two additional sources occur approximately  $60^\circ$  north and south of the ecliptic, the north and south toroidal sources (Elford & Hawkins 1964; Jones & Brown 1993).

Because of the geometry of the sporadic sources, daily rates show a maximum around local dawn, and annual rates are highest in the second half of the year for Northern hemisphere observers (e.g. Vogan & Campbell 1957). To determine the true variation of sporadic flux with time, the observing geometry of each source must be considered. Early attempts at this were made by Weiss (1957), who corrected Southern hemisphere radar meteor rates assuming both a uniform spread in radiant and an ecliptic distribution of radiant: he and others (summarized in McKinley 1961) found that rates were highest in the second half of the year. These analyses did not have the advantage of knowing the distribution of sporadic

meteor radiants, which is far from uniform, and are therefore of limited usefulness. More recently, the annual variation of the helion and antihelion sources has been studied by Poole (1997). After correcting for seasonal observing effects, he found that the helion source was most active in June, with a sharp drop in activity in July and a gradual recovery. The antihelion source had a very broad maximum in June as well, with a smaller maximum in October and no sudden changes. Poole did not attempt to measure the activity of the other sporadic sources.

We present here a preliminary analysis of our calibrated radar measurements of the strengths of the sporadic sources and their variation in time. The Canadian Meteor Orbit Radar (CMOR) in Tavistock, Ontario, Canada, was used to collect the data. While we have made an effort to correct for all observing biases, the meteor activities presented here are well defined in a relative sense but the fluxes have been scaled to an average of unity – more work on the correction factors being needed before reliable absolute fluxes can be determined.

## 2 OBSERVATIONS

This study is based on observations made at 29.85 MHz with the CMOR system (Jones et al. 2005). The directions of the radar echoes are measured typically to an accuracy of  $1^\circ$  with the five-element interferometer described by Jones, Webster & Hocking (1998). Echoes on the system are automatically detected by software (Hocking, Fuller & Vandeppeer 2001). The data analysed here was taken from 2002 May (when a power measuring system was installed at the radar) to 2005 June. The monitoring system records the power every minute and the average power over the day was used in the present analysis. In general, the daily variation in power was less than 2 per cent. Data taken prior to 2002 May were examined, but the power fluctuated too much to make those data useful for rate calculations.

The peak transmitter power of each radar varied between 5 and 6 kW. The pulse repetition frequency (PRF) was 532 Hz, and the pulses were tapered in shape and 75- $\mu$ s long. The minimum power

<sup>★</sup>E-mail: margaret.campbell@uwo.ca

detectable on the receivers was approximately  $5 \times 10^{-16}$  W; the bandwidth of the receivers was set to 25 kHz. Observations made on 901 d when the transmitter was fully operational were used to calculate fluxes. A total of 4.7 million sporadic echoes were considered, an average of 5200 d<sup>-1</sup>.

### 3 ISOLATION OF THE SOURCES

Since we wish to determine the annual variation of each of the sporadic sources, we need to be able to isolate the activity of each source from the rest of the sporadic meteor activity. In principle it is possible to use the multistation technique that yields the orbits of individual meteoroids; but for this to yield reliable results in this sort of study, the tropospheric conditions need to be such that the efficiency of the links to the remote stations must be constant throughout the year. For CMOR they are not, so that the apparent activity of a given source depends on the degree of tropospheric ducting at the frequency used by the links. Correction for this effect is difficult and we have used single-station observations to avoid this complication. Since the single-station observations do not provide the orbits of individual meteoroids, we have to recover the activity of each sporadic source from the observed distribution of echo directions. The specular (mirror-like) reflection condition dictates that the direction of the echo observed at the radar from a meteor train is perpendicular to the axis of the train.

The method used in this study is based on that described by Morton & Jones (1982). The echo directions,  $E_i$ , for meteoroids emanating from a point radiant fall on a great circle whose pole is the radiant by virtue of the specular condition. Thus by counting those echoes that are perpendicular to a given radiant,  $T_j$ , within a specified angle we might expect to obtain a measure of the strength of the radiant,  $S_j$ . We can write this mathematically

$$S_j = \sum_i w(T_j \cdot E_i) F(T_j, E_i), \quad (1)$$

where the summation is taken over all the echoes and  $F(T_j, E_i)$  is unity if the specified radiant is above the horizon at the time of occurrence of the  $i$ th meteor echo but zero otherwise and

$$w(x) = \begin{cases} 1 & \text{for } |x| < x_0, \\ 0 & \text{for } |x| \geq x_0. \end{cases} \quad (2)$$

The quantity  $x_0$  specifies how strictly we enforce the specularity criterion and is typically taken at least  $2 \sin(r_s)$ , where  $r_s$  is the rms radius of the source. We image the radiant activity over the accessible regions of the celestial sphere at many points using equation (1).

However, since any point on the great circle could be associated with any radiant perpendicular to it, the apparent strength of the radiant measured in this way depends not only on the strength of primary radiant but also, to a lesser degree, on the other radiants that are active at the same time. In imaging terms, the procedure yields images of point radiant sources as having a very diffuse halo. Jones & Jones (2005) have shown how this difficulty can be overcome by using a different convolution function. In this study, we used an earlier function for  $w(x)$  that is not as computationally efficient as that of Jones and Jones but has almost identical behavior:

$$w(x) = e^{-(x/x_0)^2/2} (1 - (x/x_0)^2). \quad (3)$$

With this function a point radiant produces an image of approximate radius  $\arcsin(x_0)$ . The apparent activity of the source depends on both the source radius and on the adopted value of  $x_0$  such that only when  $\arcsin(x_0) \gg r_s$  is the apparent strength a good measure of the true source strength.

According to Jones & Brown (1993), the sporadic sources typically have a radius in the range of  $10^\circ$ – $20^\circ$ , and we have taken  $x_0 = 0.259$  corresponding to about  $15^\circ$  in Figs 3–6 that show sporadic radiant activity plots for each month with the major showers removed.

### 4 ANALYSIS

To calculate flux (the number of meteoroids per unit area, per unit time), we take the daily meteor rate and divide by the radar collecting area. This basic flux value must also be corrected for observing biases; the process is described below. Attempts have been made to address the major observing biases, particularly those that affect each source differently, including collecting area and the initial radius effect, so that the relative activity of the sources can be compared. The total flux has been scaled so that the average value is unity, and each source has been scaled by the same factor. Absolute fluxes must wait until accurate estimates of each correction factor become available. Although the results of this study strictly apply only to a limiting magnitude of between +8 and +9, the orbital evolution work of Brown & Jones (1998) has shown that after a few revolutions since ejection from the parent comet, the dispersion of meteoroid streams is governed overwhelmingly by planetary gravitational perturbations so that the variations in position and relative source strength should be essentially independent of mass and our results should apply over a large mass range.

Five sporadic sources – the helion, antihelion, north and south apex and north toroidal – were used in this analysis. The presence of each source, and its position as a function of time, was measured each day from 29-MHz data. The variation in the position of each source from its average position is typically only a few degrees and repeats consistently from year to year, with the heliocentric longitude of the north apex source showing the greatest year-to-year changes. The measured position of the centre of each source over the 3 yr is given in Fig. 1.

The activity analysis was done using a radius of  $25^\circ$  for each source, though artificial limits were set where the sources would otherwise run into one another. This ensured that no meteors originating from the source were excluded, though some background might be included for each source. The shape of the activity curves was identical to the same analysis done at  $15^\circ$  resolution, except in the case of the north toroidal source, where the rates in May and June varied considerably. Density plots for each month, with major showers removed (Figs 2–5) show the reason: there is a diffuse source next to the north toroidal source during May and June which contributes to the  $25^\circ$  rate but not to the  $15^\circ$  rate. No attempt was made to remove this source; it was simply counted as part of the north toroidal source.

Showers were subtracted if they showed up strongly in the rate plots for each source. Some stronger showers, such as the Orionids, were not removed because they were not close enough to the sources to affect the counts. In the helion source, the Arietids were the strongest peak, with the Daytime Sextantids also visible. The antihelion source was affected by the Geminids and the South Delta Aquarids (the North Delta Aquarids were negligible). The Eta Aquarids showed strongly in the north apex source, with the Perseids also making a small contribution. The north toroidal source was strongly affected by the Quadrantids. The south apex source, observable for less than 6 months, showed no significant shower activity. For each of the showers mentioned, the radiant and radiant drift were determined from the data, and all echoes within  $3^\circ$  of the appropriate radiant were removed. This also removed any

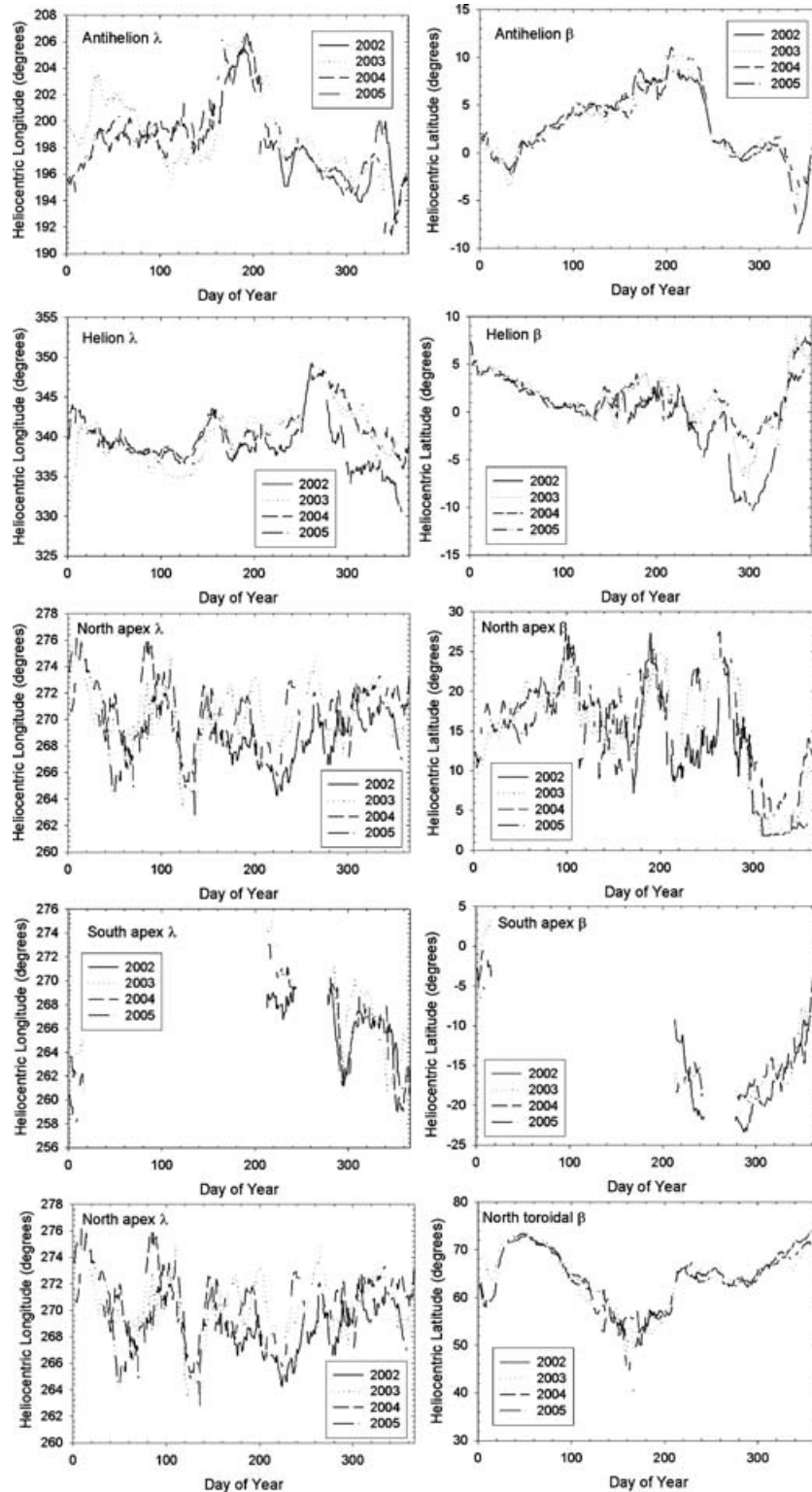


**Figure 1.** Motion of the sporadic radiants;  $\lambda$  is the heliocentric longitude, and  $\beta$  the heliocentric latitude.

sporadic meteors which happened to occur in these regions; to account for this, the background activity in the appropriate region of each source was measured before and after the shower; this background rate (corrected for any changes in transmitter power) was added to the source rate before the flux was calculated.

To convert the echo rate associated with a given radiant into flux, we need the effective collecting area of the radar to that radiant. The theory for this sort of conversion was laid down by Kaiser (1960). The specular points from which the echoes from the meteor train originate are confined to two planes, the first being the

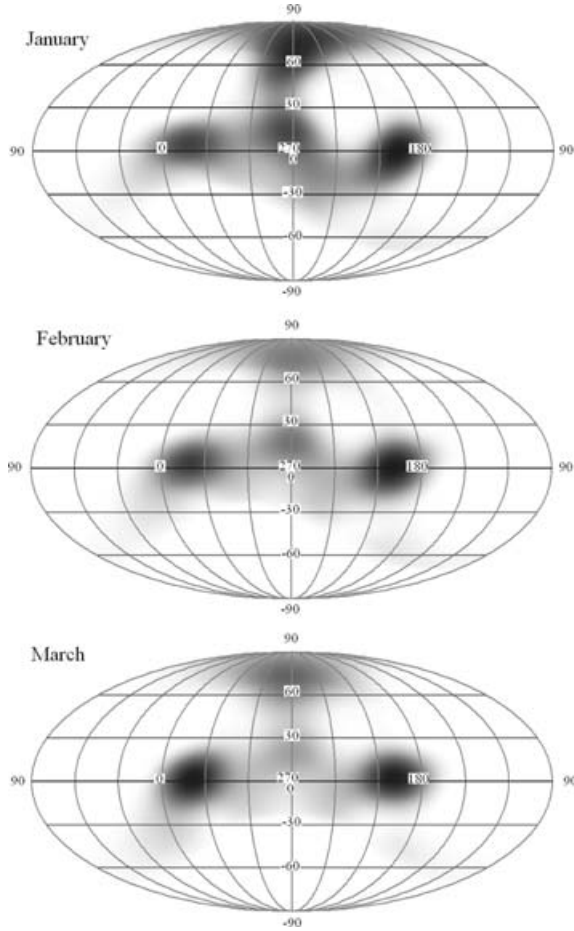


**Figure 2.** Radiant density plots, in heliocentric coordinates, for January–March. The origin is the apex of the Earth’s way, and the sun is at (0, 0).

100-km surface and the second the plane perpendicular to the radiant. The intersection of these planes is a line that Kaiser calls the echo line. Since the meteor trains have a finite vertical extent the line is actually a strip. According to Kaiser’s theory, the collecting area,  $A$ , is given by

$$A = \frac{L_v(s) \cos(z)^{s-1}}{\sin(z)} \int (q_0/q)^{s-1} dl, \quad (4)$$

where  $L_v(s)$  is the mean vertical detectable train length as a function of the echo amplitude distribution index,  $s$ ;  $z$  is the zenith angle,  $q$  is the minimum detectable electron-line density at a point on the echo line,  $q_0$  is the minimum value of  $q$  on the echo surface and where the integral is taken along the echo line.

We have made only a slight modification to Kaiser’s original theory that was based on classical single-body ablation theory by assuming the ionization curve mirrors the average luminosity curve for Low-Light-Level-Television meteors found by Fleming, Hawkes & Jones (1993).

We assume  $s = 2.0$  for all of the sporadic sources.

The collecting area can vary considerably as the sporadic sources move across the sky, and Fig. 6 shows how the collecting area averaged over the day varies with the declination of the source.

In future, these fluxes will be corrected for the limiting sensitivity of the radar and for the diffuseness of the sporadic sources. They do not need to be corrected for geometrical factors, as described in Grün et al. (2001). Geometrical corrections need to be applied for

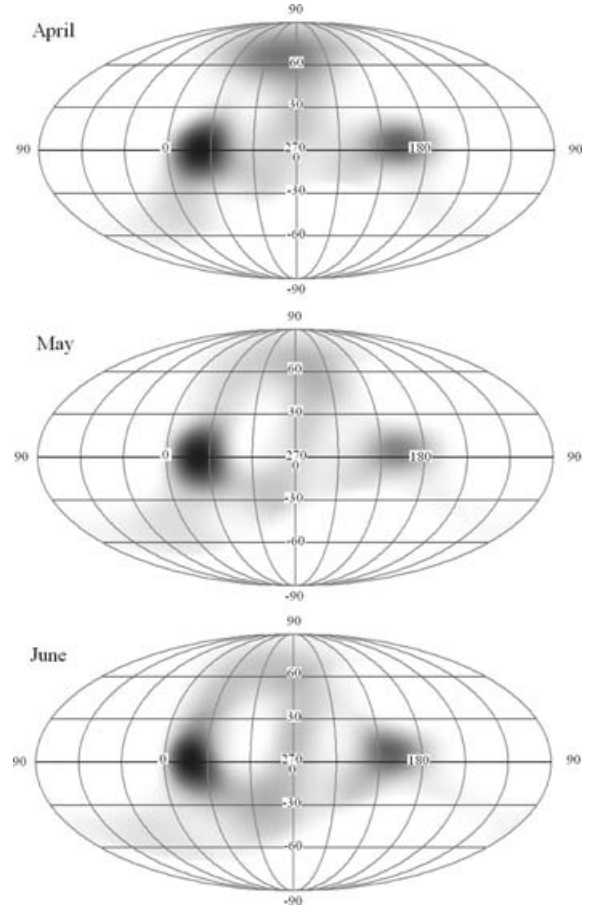


**Figure 3.** Radiant density plots, in heliocentric coordinates, for April–June.

flat plates in isotropic fluxes or spinning plates with monidirectional fluxes. In this case, we have used only those times when the radiant was above the horizon to calculate the collecting area, therefore, approximating a flat plate pointing at the radiant.

A correction was applied to account for the initial radius effect; this effect is significantly different for the various sources, and so needs to be included before a total activity can be measured. This is the least understood of the correction factors, and there is still work to be done in understanding this effect. It affects underdense echoes occurring high in the atmosphere, where the density of the air is lower: the ionized train of the meteor spreads quickly, and when its radius is comparable with the radar’s wavelength, there is destructive interference which attenuates the echo. Because faster meteors ablate higher in the atmosphere, they are affected more than slower meteors, so the apex sources (with average speed around  $60 \text{ km s}^{-1}$ ) are most attenuated. The correction factor used was that of Jones & Campbell-Brown (2005) based on the analysis of  $10^4$  sporadic meteors observed with the 29- and 38-MHz CMOR radars.

## 5 RESULTS

It was assumed in calculating the total sporadic rate that the sources were symmetrical about the ecliptic: the north and south apex sources being equal, and the north and south toroidal likewise. The north toroidal source was doubled in calculating the total, and the north apex was as well for the period when the collecting area of the south toroidal source was too small. While the variations in the

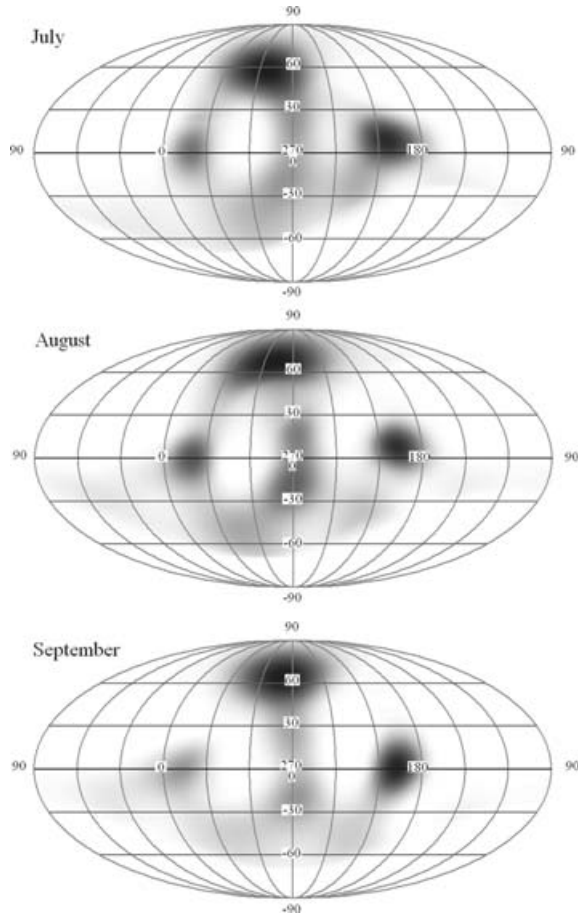


**Figure 4.** Radiant density plots, in heliocentric coordinates, for July–September.

north toroidal source are not likely to be precisely reproduced in the south toroidal, the average flux is probably similar. Each source, and the total activity, has been scaled so that the average total flux is unity. This means that the relative strengths of the sources can meaningfully be compared, but the activities do not correspond to absolute fluxes.

The total activity of sporadic meteors, as measured at 29 MHz, is given in Fig. 7. Each point represents 1 d of data, with the rate corrections described above. The activity of each of the sporadic sources is shown in Figs 8–12.

## 6 DISCUSSION

The fluxes given here are scaled to unity, and not given as absolute fluxes, for each of the sources for a number of reasons. The mass distribution index of these sources is critical to calculations of the collecting area and limiting magnitude corrections, and must be measured for each source. The CMOR radar is not currently able to measure mass distribution index since it presently depends on proprietary software optimized for the measurement of winds in the meteor region that rejects echoes that are not suitable for that purpose.

The corrected rates are very consistent from year to year for each source, which gives confidence in the procedures which correct for radar power. The helion source shows the most variation from year to year; the rates at the end of 2002 and the beginning of 2003 are

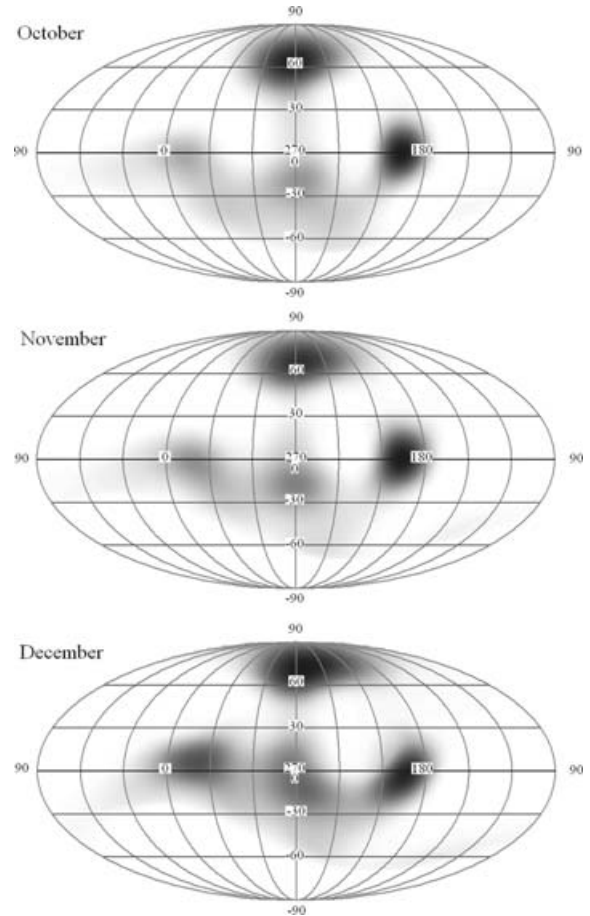


**Figure 5.** Radiant density plots, in heliocentric coordinates, for October–December.

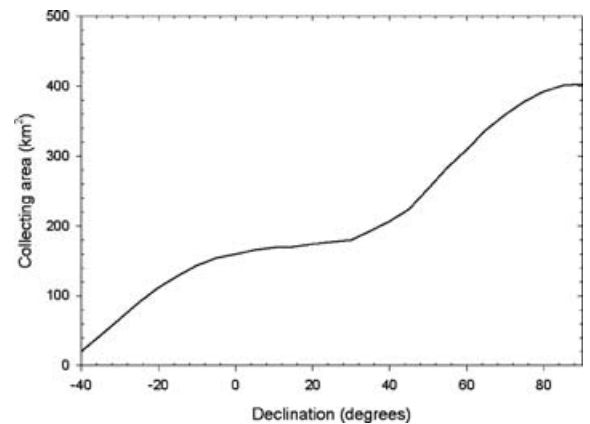


**Figure 6.** Average daily collecting area for 29-MHz radar, as a function of radiant declination. The calculation was made assuming the mass distribution index  $s = 2.0$ .

noticeably lower than in later years. The north toroidal and north apex sources show a similar effect in the fall of 2002, though less pronounced than in the case of the helion source. These discrepancies may be due to daytime ionospheric effects related to the solar maximum, which occurred in 2000. Solar activity was still high in 2002, and has been declining since then. It will be interesting

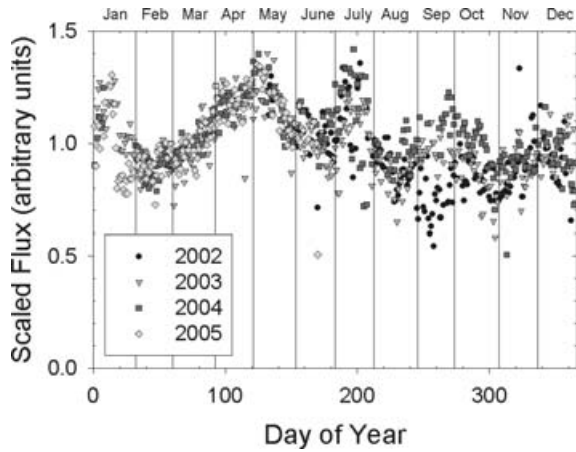


**Figure 7.** Activity of all sporadic sources as measured at 29 MHz, 2002–2005.

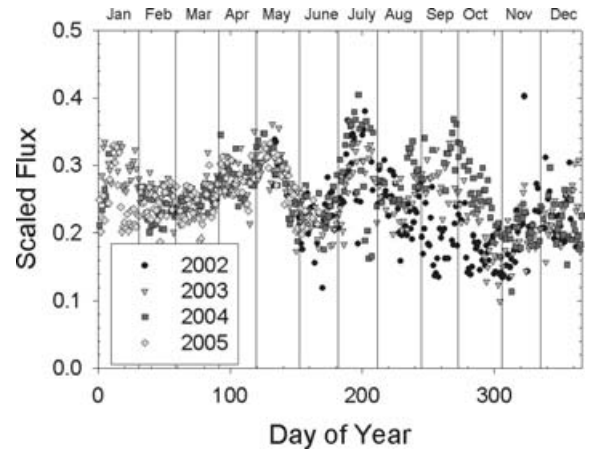


**Figure 10.** Activity of north apex source at 29 MHz, 2002–2005.

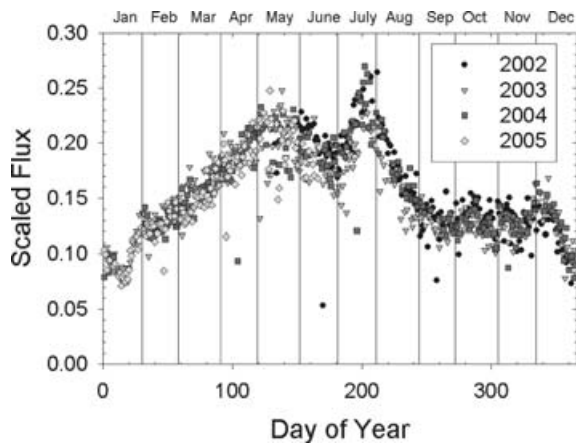


**Figure 8.** Activity of antihelion source at 29 MHz, 2002–2005.

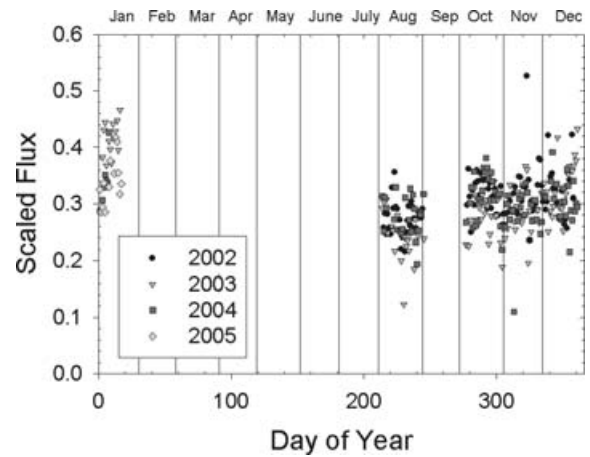


**Figure 11.** Activity of south apex source at 29 MHz, 2002–2005.

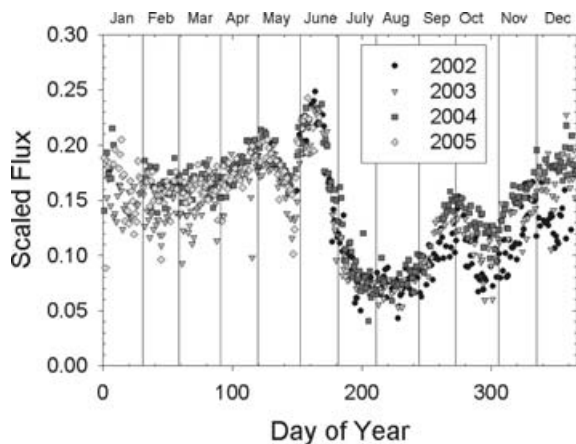


**Figure 9.** Activity of helion source at 29 MHz, 2002–2005.

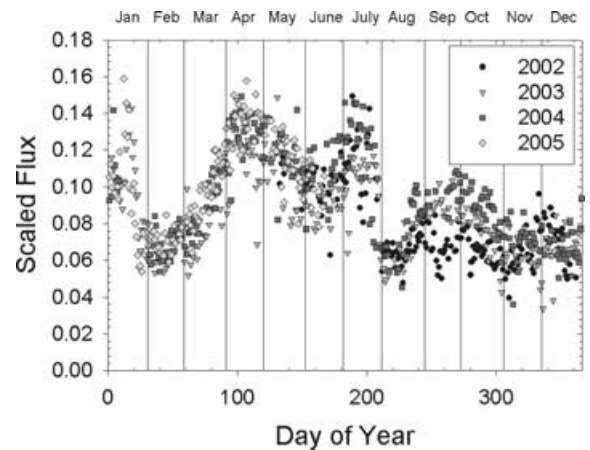


**Figure 12.** Activity of north toroidal source at 29 MHz, 2002–2005.

to investigate this effect further when data is available for a larger fraction of the solar cycle.

The total flux results do not agree with early calculations of sporadic meteor rates (e.g. Weiss 1957): the current study finds that the flux is slightly higher in the first half of the year. This difference may be due to the use of incorrect sporadic radiant distributions

in the correction of historical data, or to the difficulty in removing showers from radar data with no radiant information.

The average activity of the antihelion source appears about 10 per cent greater than the activity of the helion source. This is most likely a result of ionospheric effects, such as Faraday rotation, which affect daytime meteors but not those that occur at night. The

south apex source also appears slightly more active than the north apex source, but there is insufficient annual coverage to be certain. The north toroidal source is very prominent in the radiant maps, but is the least active source; its prominence in the uncorrected data is due to its large daily collecting area, since it is above the horizon almost the whole of every day.

The variations in the helion and antihelion sources are of particular interest, especially the precipitous drop in the helion rates between June and July. This drop does not result from instrumental or data processing effects, since it can clearly be seen in the work of Poole (1997), obtained with different techniques on a different radar in the opposite hemisphere. Ionospheric causes have been considered, but these should also affect the north toroidal source, which is visible much of the day. The effect cannot be seasonal, since it occurs at the same solar longitude in the Northern and Southern hemispheres. There must therefore be a true asymmetry in the orbital distribution of the helion source. The antihelion source shows the same order of magnitude variation, but does not have such a precipitous change. This source also agrees broadly with Poole's results, except for the October peak which is absent in our data. No showers were removed from the antihelion source in October, so the reason for its absence is not known.

Both the helion and antihelion sources have orbits consistent with short-period comets (Jones, Campbell & Nikolova 2001); the helion source represents nodes which occur post-perihelion, and the antihelion consists of pre-perihelion nodes. The fact that they do not have the same sort of variation with a change in phase argues for a small number parent bodies dominating the production of these meteoroids. This is consistent with the suggestion by Whipple, Southworth & Nilsson (1967) and later expanded by Štohl (1987) concerning comet Encke as the major source for much of the sporadic complex. The large change in activity over the year must be due to a real difference in the density of nodes in these sources with changing solar longitude; the precise changes in the activity might be used to characterize the comet population which contributes to these sources. A more detailed study of the orbits of these sources, and the change in orbital parameters through the year, would allow these meteoroid populations to be modeled dynamically.

The north apex source shows less total variation, but has noticeable peaks which repeat year after year. The strength of the source is higher than the helion and antihelion source, reflecting the higher probability of observing apex meteors, which are on average nearly twice as fast as helion/antihelion or toroidal meteors; the limiting mass for the apex sources is therefore much less than the limiting mass of the other sources. The two apex sources are most affected by the initial radius effect, so small changes in that correction factor may lead to large corrections in the apex source fluxes. The south apex source is not clearly observable for most of the year, so no conclusions can be drawn from its activity.

The north toroidal activity curve was the only one which changed shape with changing source radius in the analysis: at 15° radiant resolution, there was a drop in the rates in May and June, which disappeared at 25° resolution. This appears to be due to a broad source, not corresponding to any known shower, which appeared next to the north toroidal source. It does not show up in shower analysis of the data, since the radiant is broad (at least 10°). It could not be removed with the showers, because of its diffuseness, so it was counted as part of the north toroidal source. This source emphasizes that there is a continuum between shower and sporadic meteors: most showers occur in the region of a sporadic source and have similar orbital characteristics.

The results presented above will be of great value in determining the origin of each sporadic meteor source. Štohl (1983), using radar and photographic observations of the helion and antihelion sources, concluded that both sources were due to a single set of particles, with a 65° spread in apsides, which accounted for the apparent peak of the helion source between April and June, and the antihelion peak 4 or 5 months later, from October to December. In fact, when showers are removed, the peaks of the two sources occur much closer together, and show very different characteristics. The two sources may indeed be associated with comet 2P/Encke, as Štohl suggests, but the orbital distribution is more complicated than he assumed.

Andreev (1992) looked at apex source meteors with retrograde orbits and small semimajor axes. These types of orbits are unlike asteroids (because of their inclinations greater than 90°), but not close to any known short-period comets (because of their small eccentricities). He concluded that this group originates with Kreutz group comets, which have very small perihelia.

In this work, we have determined how the positions and activities of the sporadic sources vary throughout the year. In future works, we will examine the position and width of the sporadic sources using orbital data from the CMOR radar. We will also consider the issue of whether to divide the apex source in two, or consider only one source in the area. In some months (February or October, for example), either the north or south apex source is visible alone; in other months, both are visible, but not clearly separated. Other attenuating effects which affect radar data, such as Faraday rotation and the finite velocity effect, should also be considered: Faraday rotation may be the cause of the lower activity of the helion source compared to the antihelion. No attempt was made to correct for overdense echoes excluded from the analysis: a redesign of the filter would allow these echoes to be measured. The speed distribution of each source will be examined in detail using the orbital capabilities of the radar, and the mass distribution of the sources will be investigated with radar and optical methods.

## ACKNOWLEDGMENTS

Thanks to Zbigniew Krzeminsky, for his work in keeping CMOR operational, and to I. Williams, for helpful comments at the review stage.

## REFERENCES

- Andreev V. V., 1992, Proc. Asteroids, Comets, Meteors 1991. Lunar and Planetary Inst., Houston, p. 5
- Brown P., Jones J., 1998, *Icarus*, 133, 36
- Elford W. G., Hawkins G. S., 1964, Smithsonian. Astrophysics Observatory Research Report No. 9. Smithsonian Inst. Astrophys., Cambridge, Mass
- Fleming B. D. E., Hawkes R. L., Jones J., 1993, in Štohl J., Williams I. P., eds, *Meteoroids and their Parent Bodies*. Astronomical Institute, Slovak Academy of Science, Bratislava, p. 261
- Grün E., Baguhl M., Svedhem H., Zook H. A., 2001, in Grün E., Gustafson B., Dermott S., Fechtig H., eds, *Interplanetary Dust*. Springer-Verlag, Berlin, p. 295
- Hawkins G. S., 1956, *MNRAS*, 116, 92
- Hocking W. K., Fuller B., Vandepeer B., 2001, *J. Atmos. Terr. Phys.*, 63, 155
- Jones J., Brown P., 1993, *MNRAS*, 265, 524
- Jones J., Campbell-Brown M., 2005, *MNRAS*, 359, 1131
- Jones J., Jones W. 2005, *MNRAS*, in press
- Jones J., Webster A. R., Hocking W. K., 1998, *Radio Sci.*, 33, 55
- Jones J., Campbell M., Nikolova S., 2001, in Warmbein B., ed., *Proc. Meteoroids*. ESA Publications, Noordwijk, p. 575

- Jones J., Brown P., Ellis K., Webster A., Campbell-Brown M., Krzeminski Z., Weryk R., 2005, *Planet. Space Sci.*, 53, 413  
Kaiser T., 1960, *MNRAS*, 121, 284  
McKinley D. W. R., 1961, *Meteor Science and Engineering*. McGraw-Hill, New York  
Morton J. D., Jones J., 1982, *MNRAS*, 198, 737  
Poole L. M. G., 1997, *MNRAS*, 290, 245  
Sekanina Z., 1976, *Icarus*, 27, 265  
Štohl J., 1983, *Proc. Asteroids, Comets, Meteors*. Astron. Observ., Uppsala, p. 419  
Štohl J., 1987, *A&A*, 187, 933  
Vogan E. L., Campbell L. L., 1957, *Can. J. Phys.*, 35, 1176  
Weiss A. A., 1957, *Aust. J. Phys.*, 10, 77  
Weiss A. A., Smith J. W., 1960, *MNRAS*, 121, 5  
Whipple F. L., Southworth R. B., Nilsson C. S., 1967, *SAO Special Report No. 239*. Smithsonian Inst. Astrophys., Cambridge, Mass.

This paper has been typeset from a  $\text{\TeX}/\text{\LaTeX}$  file prepared by the author.